

limiting box chord and box aspect ratio. On the other hand, it will permit paneling of delta wings with little effort and without violating the guidelines. A limit of one-quarter of a wavelength on both the spanwise and chordwise extent of a doublet line is suggested to ensure reasonably linear convergence behavior with respect to simultaneous refinement of spanwise and chordwise paneling.

References

- ¹Albano, E., and Rodden, W. P., "A Doublet-Lattice Method for Calculating Lift Distributions on Oscillating Surfaces in Subsonic Flows," *AIAA Journal*, Vol. 7, No. 2, 1969, pp. 279–285.
- ²Rodden, W. P., Giesing, J. P., and Kalman, T. P., "New Developments and Applications of the Subsonic Doublet-Lattice Method for Nonplanar Configurations," AGARD, CP-80-71, Nov. 1970 (Paper 4).
- ³Rodden, W. P., and Johnson, E. H., *MSC/NASTRAN Aeroelastic Analysis User's Guide*, The MacNeal-Schwendler Corp., Los Angeles, CA, 1994.
- ⁴Rodden, W. P., Taylor, P. F., and McIntosh, S. C., Jr., "Further Refinement of the Nonplanar Aspects of the Subsonic Doublet-Lattice Lifting Surface Method," International Council of the Aeronautical Sciences, Paper 96-2.8.2, Sept. 1996.
- ⁵Rodden, W. P., Taylor, P. F., McIntosh, S. C., Jr., and Baker, M. L., "Further Convergence Studies of the Enhanced Subsonic Doublet-Lattice Oscillatory Lifting Surface Method," *Proceedings of the International Forum on Aeroelasticity and Structural Dynamics* (Rome, Italy), Vol. III, Associazione Italiana di Aeronautica ed Astronautica, Rome, Italy, 1997, pp. 401–408.
- ⁶Van Zyl, L. H., "Arbitrary Accuracy Integration Scheme for the Subsonic Doublet Lattice Method," *Journal of Aircraft*, Vol. 35, No. 6, pp. 975–977.
- ⁷Von Kármán, T., and Sears, W. R., "Airfoil Theory for Non-Uniform Motion," *Journal of the Aeronautical Sciences*, Vol. 5, No. 10, 1938, pp. 379–390.
- ⁸Laschka, B., "Zur Theorie der harmonisch schwingenden tragenden Flächen bei Unterschallanströmung," *Zeitschrift für Flugwissenschaften*, Vol. 11, No. 7, 1963, pp. 265–292.
- ⁹Desmarais, R. N., "An Accurate and Efficient Method for Evaluating the Kernel of the Integral Equation Relating Pressure to Normalwash in Unsteady Potential Flow," AIAA Paper 82-0687, May 1982.

Rapid Prediction of Wing Rock for Slender Delta-Wing Configurations

Lars E. Ericsson*
Mountain View, California 94040

Introduction

SINCE the initial experiments by Nguyen et al.¹ and Levin and Katz,² which showed that an 80-deg delta wing at high angles of attack exhibits the limit-cycle oscillations in roll, referred to as slender wing rock, Arena and Nelson^{3,5–7} and Arena et al.⁴ have been performing a series of tests and analyses of a sharp-edged 80-deg delta wing, aimed to provide insight into the fluid mechanical processes causing slender

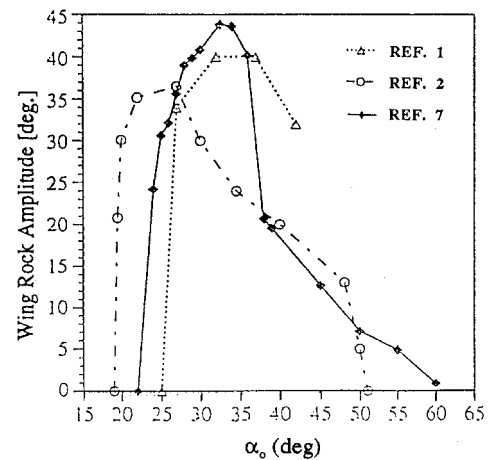


Fig. 1 Experimentally determined wing-rock-amplitude envelope for an 80-deg delta wing.

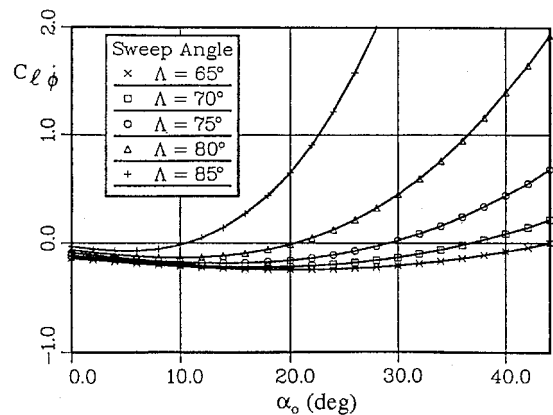


Fig. 2 Effect of leading-edge sweep on delta-wing roll damping at high angles of attack.⁹

wing rock. In Fig. 1 their experimental wing rock results⁷ are compared to those in Refs. 1 and 2. How the difference between the results in Refs. 1 and 2 was caused by the different experimental setups is discussed in Ref. 8. The likely reason that the test results in Ref. 7 show a higher maximum limit-cycle amplitude than those in Refs. 1 and 2 (Fig. 1) is that the damping provided by the bearing friction in Refs. 1 and 2 was almost completely eliminated in Ref. 7 by the use of an air bearing. The predicted start of wing rock⁹ (Fig. 2) agrees well with these friction-free test results (Fig. 1). In addition to knowing when slender wing rock will start for a particular leading-edge sweep⁹ (Fig. 2), the vehicle designer also needs to know how large the limit-cycle amplitude can become when the critical angle of attack is exceeded; e.g., $\alpha > 20$ deg for $\Lambda = 80$ deg (Fig. 2). A simple analysis for the determination of the maximum possible limit-cycle amplitude is described, which produces results that compare well with the experimental results in Fig. 1 for the 80-deg delta wing.

Maximum Limit-Cycle Amplitude

Experimental results for the 80-deg delta wing⁴ (Fig. 3a) show that when the roll angle is increased from $\phi = 0$ to the maximum wing rock value, $\phi = 44$ deg (Fig. 1), the left, laterally leeside vortex increases its distance above the wing surface from $\zeta_v = z_v/s \approx 0.47$ to $\zeta_v \approx 1.04$ while moving outboard from $\eta_v = y_v/s \approx -0.65$ to $\eta_v \approx -1.70$. Combining the ζ_v , η_v results in Fig. 3a gives the vortex location relative to the wing as a function of roll angle (Fig. 3b). The combined effects of the vortex-induced suction and downwash will contribute

Presented as Paper 98-0498 at the AIAA 36th Aerospace Sciences Meeting, Reno, NV, Jan. 12–15, 1998; received March 6, 1998; revision received July 10, 1998; accepted for publication July 13, 1998. Copyright © 1998 by Lars E. Ericsson. Published by the American Institute of Aeronautics and Astronautics, Inc., with permission.

*Consulting Engineer. Fellow AIAA.

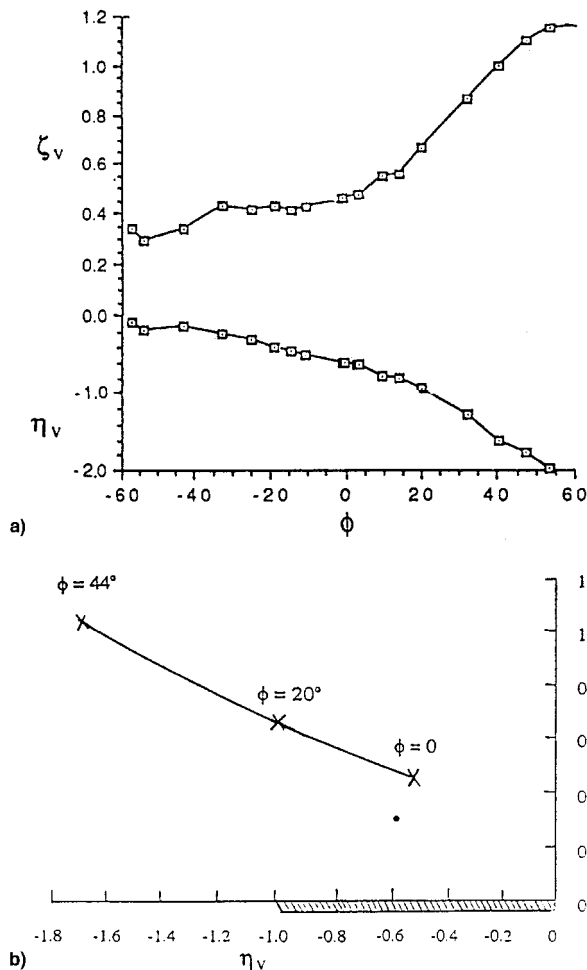


Fig. 3 Effect of roll angle on vortex position above the left, leeward side of 80-deg delta wing at $\alpha = 30^\circ$: a) measured $\eta_v(\phi)$ and $\zeta_v(\phi)$, and b) vortex position defined by $\eta_v(\phi)$ and $\zeta_v(\phi)$.

negligibly to the rolling moment on the left wing half at $\phi = 44^\circ$ compared with $\phi = 20^\circ$ and 0° . The loss of vortex-induced lift on the left, leeward wing half with increasing ϕ generates a negative, statically stabilizing contribution $(\Delta C_l)_{LV}$ to the rolling moment, which through the time lag effect becomes dynamically destabilizing.¹⁰ The conceptual variation of the loss of vortex-induced rolling moment, $-(\Delta C_l)_{LV} = f(\phi)$, is shown by a solid line in Fig. 4. The dashed line represents the approximation of the vortex liftoff characteristics that was used in Ref. 11 to determine the maximum possible wing-rock amplitude. Earlier analysis of limit-cycle oscillations in pitch of the Polaris re-entry body¹² provided convincing evidence that such an approximation would only slightly overestimate the maximum possible limit-cycle amplitude.

Based on the experience with the Polaris re-entry body,¹² an integrated measure $C_{\bar{\delta}}$ of the nonlinear roll damping was derived in Ref. 11, using the dashed-line approximation in Fig. 4. The limit-cycle amplitude $\Delta\phi_{WR}$ of the roll oscillations is defined by $C_{\bar{\delta}} = 0$. This computed wing-rock amplitude was proportional to the vortex-induced normal force C_{NV} lost on the leeward wing half through the vortex liftoff. As this vortex-induced force C_{NV} is proportional to $\sin^2\alpha$ (Ref. 13), the predicted maximum wing-rock amplitude increases very quickly with α (solid line in Fig. 5). Also shown by the dashed line in Fig. 5 is the angle of attack, $\alpha_{VB} = \tan^{-1}(\tan\alpha_0 \cos\Delta\phi_{WR})$, where vortex breakdown will start to occur on the windward half of the delta wing when accounting for the effect of $\Delta\phi_{WR}$ on the effective leading-edge sweep (α_0 is the inclination of

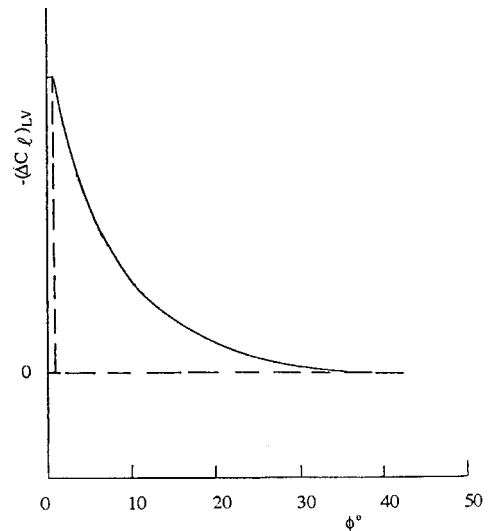


Fig. 4 Conceptual contribution to the rolling moment by the left, leeward leading-edge vortex.

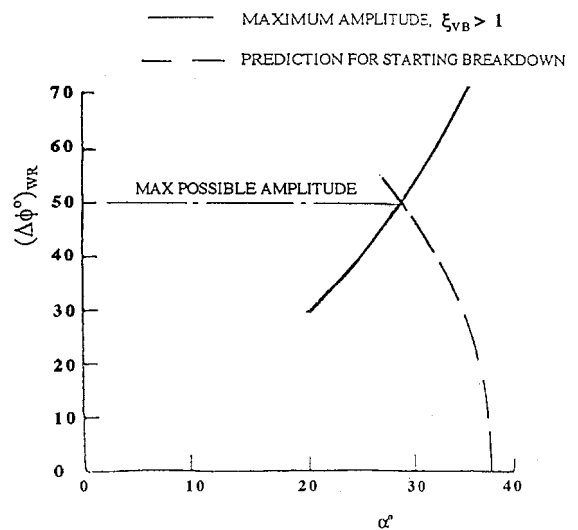


Fig. 5 Predicted maximum possible wing-rock amplitude for 80-deg delta wing.

the roll axis). In Ref. 10 it was demonstrated that the occurrence of vortex breakdown on the windward wing half generated roll damping. Furthermore, it was argued that the fast movement of vortex breakdown forward of the trailing edge¹⁴ (Fig. 6) would, on the slender delta wings prone to wing rock ($\Lambda > 70^\circ$ in Fig. 6), provide a sudden, large increase of the roll damping that would stop any further growth of the wing-rock amplitude. Figure 5 shows that the intersection of the two curves, defining the maximum possible magnitude of the wing-rock amplitude, exceeds the maximum amplitudes measured on the 80-deg delta wing^{1,2,7} (Fig. 1).

The $\alpha_0 - \theta_A$ boundary for the occurrence of slender wing rock, defined by Ref. 9 and Fig. 2, is shown in Fig. 7. The dashed portions indicate that wing rock is likely to be prevented from occurring; at $\theta_A > 18^\circ$ deg by the burst-induced damping^{11,14} (Fig. 6), and at $\theta_A \leq 7^\circ$ deg by the presence of asymmetric vortex burst¹⁵ and the roll damping generated by the associated roll trim $|\phi_0| > 0$. It is shown in Ref. 16 that for the 80-deg delta wing, $|\phi_0| = 10^\circ$ deg would generate an equivalent sideslip angle $|\beta| = 5^\circ$ deg at $\alpha = 30^\circ$. As it is likely that $|\phi_0|$ will exceed 10° deg and the experimental results¹ show that $|\beta| > 5^\circ$ deg provides roll damping for $\alpha < 35^\circ$ deg, wing rock will not occur for $\theta_A \leq 7^\circ$ deg.

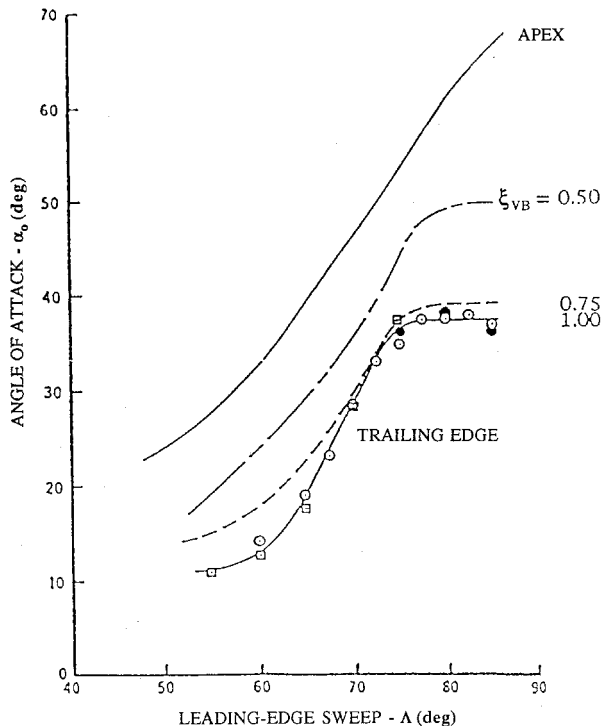


Fig. 6 Vortex breakdown position on sharp-edged delta wings.¹⁴

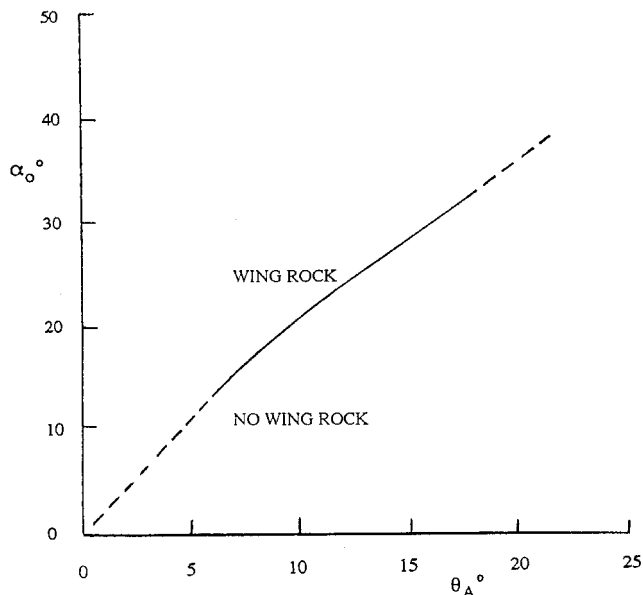


Fig. 7 Predicted wing-rock boundary for slender delta wings.

Conclusions

The information that the vehicle designer needs early in the design cycle is 1) the angle-of-attack/leading-edge-sweep range in which slender wing rock will occur and 2) the maximum wing-rock amplitude. Figure 7 provides the (α, θ_A) boundary for starting wing rock. To determine the maximum possible oscillation amplitude, one needs to repeat the computations,¹¹ producing Fig. 5 for apex half-angles θ_A different from 10 deg.

References

- ¹Nguyen, L. T., Yip, L., and Chambers, J. R., "Self-Induced Wing Rock of Slender Delta Wings," AIAA Paper 81-1883, Aug. 1981.
- ²Levin, D., and Katz, J., "Dynamic Load Measurements with Delta Wings Undergoing Self-Induced Roll Oscillations," *Journal of Aircraft*, Vol. 21, No. 1, 1984, pp. 30–36.

³Arena, A. S., Jr., and Nelson, R. C., "The Effect of Asymmetric Vortex Wake Characteristics on a Slender Delta Wing Undergoing Wing Rock Motion," AIAA Paper 89-3348, Aug. 1989.

⁴Arena, A. S., Jr., Nelson, R. C., and Schiff, L. B., "An Experimental Study of the Nonlinear Phenomenon Known as Wing Rock," AIAA Paper 90-2812, Aug. 1990.

⁵Arena, A. S., Jr., and Nelson, R. C., "Unsteady Surface Measurements on a Slender Delta Wing Undergoing Limit Cycle Wing Rock," AIAA Paper 91-0434, Jan. 1991.

⁶Arena, A. S., Jr., and Nelson, R. C., "A Discrete Vortex Model for Predicting Wing Rock of Slender Wings," AIAA Paper 92-4497, Aug. 1992.

⁷Arena, A. S., Jr., and Nelson, R. C., "Experimental Investigations on Limit Cycle Wing Rock of Slender Wings," *Journal of Aircraft*, Vol. 31, No. 5, 1994, pp. 1148–1155.

⁸Ericsson, L. E., and Beyers, M. E., "Ground Facility Interference Effects on Slender Vehicle Unsteady Aerodynamics," *Journal of Aircraft*, Vol. 33, No. 1, 1996, pp. 117–124.

⁹Ericsson, L. E., and King, H. H. C., "Rapid Prediction of High-Alpha Unsteady Aerodynamics of Slender-Wing Aircraft," *Journal of Aircraft*, Vol. 29, No. 1, 1992, pp. 85–92.

¹⁰Ericsson, L. E., "Fluid Dynamics of Slender Wing Rock," *Journal of Aircraft*, Vol. 21, No. 5, 1984, pp. 322–328.

¹¹Ericsson, L. E., "Analytic Prediction of the Maximum Amplitude of Slender Wing Rock," *Journal of Aircraft*, Vol. 26, No. 1, 1989, pp. 35–39.

¹²Ericsson, L. E., "Unsteady Aerodynamics of Separating and Reattaching Flow on Bodies of Revolution," *Recent Research on Unsteady Boundary Layers*, Vol. 1, IUTAM Symposium, Laval Univ., PQ, Canada, 1971, pp. 481–512.

¹³Polhamus, E. C., "Prediction of Vortex-Lift Characteristics by a Leading-Edge Suction Analogy," *Journal of Aircraft*, Vol. 8, No. 4, 1971, pp. 193–199.

¹⁴Wentz, W. H., and Kohlman, D. L., "Vortex Breakdown on Slender Sharp-Edged Wings," *Journal of Aircraft*, Vol. 8, No. 3, 1971, pp. 156–161.

¹⁵Stahl, W., Mahmood, M., and Asghar, A., "Experimental Investigation of the Vortex Flow on Delta Wings at High Incidence," AIAA Journal, Vol. 30, No. 4, 1992, pp. 1027–1032.

¹⁶Ericsson, L. E., "Slender Wing Rock Revisited," *Journal of Aircraft*, Vol. 30, No. 3, 1993, pp. 352–356.

Correlation for the Estimation of Afterbody Drag with Hot Jet Exhaust

N. B. Mathur*

National Aerospace Laboratories,
Bangalore 560 017, India

Introduction

MODERN turbojet and turbofan engines of combat aircraft operating over a wide range of power settings experience jet exhaust temperature typically varying from 1000–2000 K, whereas much of afterbody-nozzle testing is conducted with a cold jet near 300 K.^{1–5} Thus there remains a problem to determine the extent to which jet total temperature (and its associated gas constants) affects the afterbody drag of a combat aircraft under various operating conditions of its nozzle during the flight operation.^{6–8} Physical modeling of jet freestream interactions with temperature effects is quite difficult; and, calculations of afterbody drag with hot jet exhaust are computationally intensive. Efforts made earlier for the es-

Received Aug. 17, 1997; revision received June 6, 1998; accepted for publication June 13, 1998. Copyright © 1998 by the American Institute of Aeronautics and Astronautics, Inc. All rights reserved.

*Scientist, Experimental Aerodynamics Division. Member AIAA.